

Reprinted from

JAPANESE JOURNAL OF
**APPLIED
PHYSICS**

REGULAR PAPER

**Reduction of Nonlinear Absorption in $\text{Li}_2\text{B}_4\text{O}_7$
by Temperature- and Repetition Rate-Control**

Masakuni Takahashi, Genta Masada, Ichiro Sekine, Marilou Cadatal, Toshihiko Shimizu, Nobuhiko Sarukura, Clare Byeon, Vladimir Fedorov, Sergey Mirov, Alex Dergachev, and Peter F. Moulton

Jpn. J. Appl. Phys. **48** (2009) 112502

Reduction of Nonlinear Absorption in $\text{Li}_2\text{B}_4\text{O}_7$ by Temperature- and Repetition Rate-Control

Masakuni Takahashi, Genta Masada*, Ichiro Sekine, Marilou Cadatal¹, Toshihiko Shimizu¹, Nobuhiko Sarukura¹, Clare Byeon², Vladimir Fedorov², Sergey Mirov², Alex Dergachev³, and Peter F. Moulton³

Central Research Institute, Mitsubishi Materials Corporation, 1002-14 Mukohyama, Naka, Ibaraki 311-0102, Japan

¹Institute of Laser Engineering, Osaka University, 2-6 Yamadaoka, Suita, Osaka 565-0871, Japan

²The University of Alabama at Birmingham, 310 Campbell Hal, 1300 University Blvd, Birmingham, AL 35216, U.S.A.

³Q-Peak Inc., 135 South Road, Bedford, MA 01730, U.S.A.

Received March 30, 2009; accepted September 4, 2009; published online November 20, 2009

We address the critical issue of thermal dephasing of the UV harmonic generation process due to nonlinear absorption in $\text{Li}_2\text{B}_4\text{O}_7$ crystals. Reduction of nonlinear absorption is achieved by increasing the crystal temperature up to 200 °C and reducing the pulse repetition rate. Our results show the way for significant improvement of the conversion efficiency for the fourth harmonic generation of Nd lasers using $\text{Li}_2\text{B}_4\text{O}_7$ crystals. © 2009 The Japan Society of Applied Physics

DOI: 10.1143/JJAP.48.112502

1. Introduction

There has been a strong and continuing demand for low-cost, high-pulse energy ultraviolet (UV) laser sources for various scientific and industrial applications including a pumping source for a terawatt (TW) UV $\text{Ce}^{3+}:\text{LiCaAlF}_6$ chirped pulse amplification laser system.¹⁾ For this purpose, phase-matched, second-order, nonlinear conversion processes in borate crystals are promising. With a wide range of nonlinear crystals to choose from including beta-barium borate ($\beta\text{-BaB}_2\text{O}_4$ or BBO),²⁾ lithium triborate (LiB_3O_5 or LBO),³⁾ cesium lithium borate ($\text{CsLiB}_6\text{O}_{10}$ or CLBO),⁴⁾ and lithium tetraborate ($\text{Li}_2\text{B}_4\text{O}_7$ or LB4),⁵⁾ the choice of the suitable nonlinear optical crystal is a key issue. Large-aperture, homogeneous and easy to handle crystals are desired for high pulse energy applications. Energy scaling capability is also an important consideration in the development of pump sources for TW UV laser systems. Although both BBO and CLBO crystals have high non-linearity and high damage threshold, they have disadvantages, with CLBO being soft and highly hygroscopic; therefore requiring maintenance of specific atmospheric conditions such as temperature and humidity,^{4,6-8)} and BBO having strong two-photon absorption in the UV.^{2,9)} For LBO, the wavelength conversion range is limited (it does not have phase-matching conditions for fourth harmonic generation by direct doubling of Nd laser second harmonic) and it is difficult to grow large crystals.³⁾

LB4 is a piezoelectric borate crystal belonging to the point group of 4mm. It was originally developed as a material for surface acoustic wave (SAW) devices for electronics applications.¹⁰⁾ Compared to BBO and CLBO, LB4 crystals have such advantages as low absorption in the UV region, with transparency down to 170 nm, excellent mechanical properties, easy fabrication, and high resistance against humidity. In the past, 7-cm-diameter LB4 crystals have been successfully grown by the Czochralski method with few dislocations and with good homogeneity of the refractive index. Second-harmonic and sum-frequency generation, including the fourth and the fifth harmonics of a Q-switched Nd:yttrium aluminum garnet (YAG) laser has also been

reported.⁵⁾ With a cascade frequency-doubling scheme of a Nd:YAG laser, LB4 has been demonstrated to generate 0.43-J, 266-nm pulses at 10 Hz with a total conversion efficiency of 30.5% and good stability over 15 h.¹¹⁾ However, the LB4 crystal has a small nonlinearity and a narrow angular acceptance bandwidth. Because of these, for the same laser power, LB4 has significantly lower conversion efficiency compared to BBO and CLBO. A summary of the optical properties of these three crystals are summarized in Table I.¹²⁾ Typical ways of improving conversion efficiency include tight focusing to increase the peak power density of the incident light, increase of the crystal length, and the use of multiple crystals in walk-off-compensated arrangement. A very important factor for UV generation in LB4 is the presence of linear and/or non-linear absorption, which can limit the conversion efficiency and attainable output power/energy. Taking this into consideration, optical-quality LB4 crystal with >99.99% purity and with practically negligible linear absorption at the wavelengths of the first, second, and forth harmonics of Nd lasers (0.25–1.1 μm range) was grown (see Fig. 1). However, nonlinear absorption (NLA) effects and more complex phenomena such as dynamic absorption due to transient crystal defects (color centers) created by high intensity UV light present a fundamental problem. Creation of transient color centers due to NLA can lead to linear absorption not only at UV wavelength but also at the wavelengths of first and second harmonics. Absorption in a non-linear crystal causes non-uniform heating, which consequently decreases the UV conversion efficiency due to thermal dephasing.

2. Experiment and Results

In this paper the relationship between the crystal temperature, pulse repetition rate, and crystal absorption (particularly nonlinear absorption) is investigated. Based on the experimental results, means of reducing the effects of NLA absorption on the phase-matching conditions in LB4 crystal are proposed.

LB4 crystals of very high optical quality and high purity can be grown. Figure 1 illustrates the absorption spectrum of LB4 crystals at room temperature. This absorption data was obtained from spectrophotometer transmission measurements of two LB4 crystals with various lengths. The absorption coefficient k was determined using the formula:

*Present address: Research Institute, Quantum Information Science Research Center, Tamagawa University, 6-1-1 Tamagawa Gakuen, Machida, Tokyo 194-8610, Japan.

Table I. Optical properties of BBO, CLBO, and LB4.

Wavelength (nm)	Crystal	Cut-off (nm)	θ_{pm} (deg)	d_{eff} (pm/V)	Acceptance angle (deg cm)	Acceptance wavelength (nm cm)	Walkoff angle (deg)
532 → 266	BBO	190	48	1.32	0.010	0.07	4.80
	CLBO	180	62	0.85	0.028	0.13	1.83
	LB4	170	65	0.16	0.029	0.12	1.66

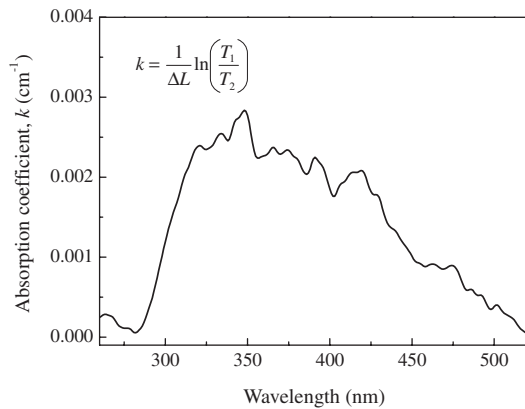


Fig. 1. Absorption coefficient of LB4 crystal in 250–600-nm spectral range at room temperature.

$$k = \frac{1}{\Delta L} \ln\left(\frac{T_1}{T_2}\right), \quad (1)$$

where T_1 is the transmission of shorter crystal (0.6 cm), T_2 is the transmission of longer crystal (3 cm), and ΔL is the crystal length difference (2.4 cm). Such procedure allows us to determine the absorption coefficient without knowledge of the refractive index and its dispersion (to account for Fresnel losses in transmission measurements). As one can see the absorption coefficient in 250–600 nm range does not exceed $\sim 0.005 \text{ cm}^{-1}$ throughout the measured spectral range. A similar absorption coefficient was obtained in a single-wavelength measurement using 262-nm laser radiation.

For low-repetition-rate studies we utilized the second and fourth harmonic radiation of a Q-switched, 10-Hz Nd:YAG laser with a pulse duration of 5 ns. On the other hand, we used a Nd:YLF laser operated at 1, 10, and 30 kHz, with pulse durations of 33, 45, and 58 ns, respectively, for high-repetition-rate experiments. The temporal profiles of the pump pulses were detected using an Si detector with a time response of less than 400 ps. The NLA coefficient was characterized using the z -scan technique.^{13,14} The LB4 crystal was translated in the z -direction of a focused Gaussian beam by a computer-controlled actuator, which was synchronized with all the detectors. Pyroelectric joule meters and an Si photodetector were used for all pulse energy measurements. The pump energy could be controlled by a variable attenuator consisting of a half-wave plate and a Glan prism. Two focusing lenses with 18 and 45 cm focal lengths were alternatively used throughout the procedure. Spatial energy distributions of the fourth-harmonic radiation on the focusing lenses were determined by a standard knife-edge method and within measurement errors coincide with the beam diameter calculated from fitting the z -scan data. The beam radius was 11 μm for the 18 cm lens, while it was 35 μm for the 45 cm lens. On the other hand, the spatial energy

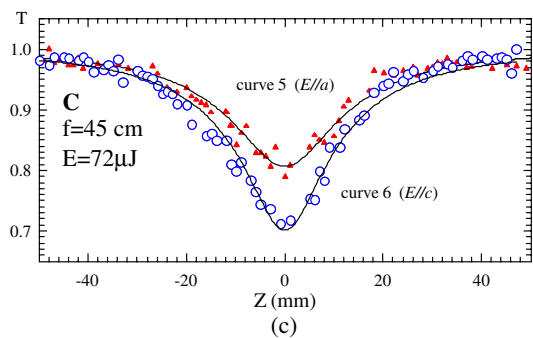
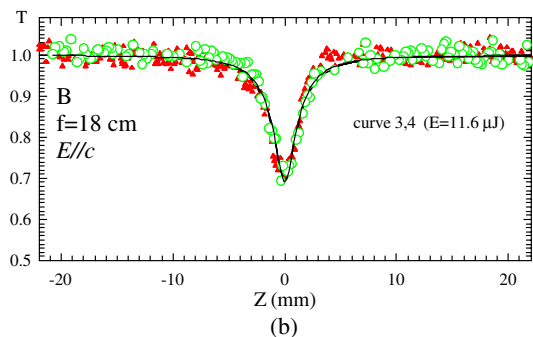
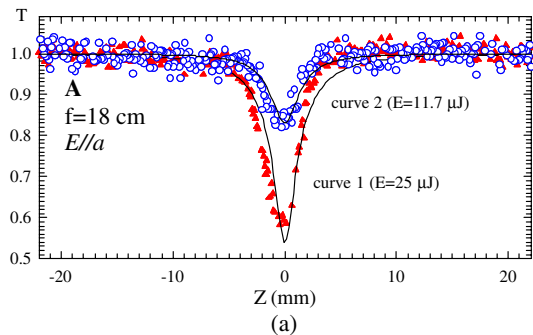


Fig. 2. (Color online) Open aperture z -scan measurements in LB4 crystals at RT using low repetition rate 266-nm pulsed laser excitation source for different lenses, incident beam intensity and light polarization: (a) z -scan transmission at two different pulse energies with light polarization parallel to the a -axis ($E \parallel a$). (b) z -scan transmission at two different spots in the crystal with light polarization parallel to the c -axis ($E \parallel c$). (c) z -scan transmission for two orthogonal polarizations of laser excitation $E \parallel a$ (curve 5) and $E \parallel c$ (curve 6). The parameters pertaining to the curves are summarized in Table II.

distribution of the second-harmonic radiation was calibrated using the z -scan data of CS_2 as a calibration sample. In order to investigate the influence of temperature on NLA, the LB4 crystal was set in a temperature-controlled mount.

z -scan data at 266 nm in a 3-mm-thick LB4 sample measured using different lenses, incident beam intensity and light polarization is depicted in Figs. 2(a)–2(c). The data in Fig. 2(a) (curves 1 and 2) was obtained at two different pulse energies with light polarization parallel to the a -axis ($E \parallel a$). Curves 3 and 4 [Fig. 2(b)] were measured under the same conditions in different crystal spots and the difference

Table II. Parameters used in fitting the experimental z-scan curves at 266 nm shown in Fig. 2.

Focal length, F (cm)	Energy, E (μJ)	NLA, β (m/W) $\times 10^{11}$	Intensity, I_0 (GW/cm^2)	Spot size, w_0 (μm)	Transmittance, ΔT (%)	Polarization	Curve
18	11.7	1.8	1.1	11.04	17	$E \parallel a$	1
18	25	2.1	2.2	11.07	55	$E \parallel a$	2
45	72	2.9	0.8	33	20	$E \parallel a$	5
18	11.6	3.0	1.3	10.84	30	$E \parallel c$	3
18	11.6	2.8	1.3	10.48	30	$E \parallel c$	4
45	72	4.0	0.9	35	30	$E \parallel c$	5

between the curves was less than the uncertainty of the measurements. Figure 2(c) shows that the LB4 crystal possesses a noticeable anisotropy of NLA. The normalized transmittance is related to the NLA coefficient by

$$T(z) = \sum_{m=0}^4 \frac{(-q_0)^m}{(1 + z^2/z_0^2)^m (m+1)^{3/2}}, \quad (2)$$

where $q_0 = \beta I_0 L_{\text{eff}}$, $L_{\text{eff}} = (1 - e^{-\alpha L})/\alpha$, α is the linear absorption coefficient, L_{eff} is the effective length, and I_0 is the peak intensity at the focal point ($z = 0$). All experimental curves were fitted using four terms of the nonlinear regression relating the NLA process with open aperture z-scan transmission measurements. The parameters used are summarized in Table II. The nonlinear absorption coefficient, β , and the beam radius, w_0 , were also used as fitting parameters.

A set of experiments performed at 532 nm showed that LB4 does not exhibit any NLA in this wavelength region.

Similar z-scan measurements were performed for a BBO crystal with a thickness of 7 mm and cut at 49° angle. From eq. (2) relating the normalized transmittance to the nonlinear absorption coefficient, there are the relation as

$$\Delta T \approx \frac{z I_0 \beta}{2\sqrt{2}}, \quad (3)$$

where ΔT is defined as the difference between the maximum and the minimum transmission in z-scan curves measured at different levels of excitation pulse energy and z is crystal length. The following ratio of the NLA for BBO and LB4 can be derived from eq. (3):

$$\frac{\beta_{\text{BBO}}}{\beta_{\text{LB4}}} \approx \frac{(\Delta T/E)_{\text{BBO}} L_{\text{LB4}}}{(\Delta T/E)_{\text{LB4}} L_{\text{BBO}}} = \frac{0.5}{0.093} \times \frac{3}{7} = 2.3, \quad (4)$$

where E is the energy of laser pulse.

Equation (4) shows that NLA in BBO crystal is approximately twice-larger than that of the LB4 crystal (see Fig. 3). For reference the incident beam diameter used in the experiments is from 43 to 64 mm and is within Raleigh range. Moreover the incident beam diameter is the same for both BBO and LB4 experiments. It is in good agreement with the previously reported two-parabolic band model.¹⁵⁾ According to this model, the third order susceptibility is proportional to inverse cube of energy gap. It is also observed that the anisotropy of NLA coefficient in LB4 crystal is comparable with that in BBO crystal.

We studied the dependence of the LB4 NLA coefficient vs the crystal temperature in the range from room temperature (RT) up to 200°C at different repetition rates. Figure 4 shows the dependence of NLA in LB4 vs the pulse repetition rate. As one can see, temperature has no effect on the value

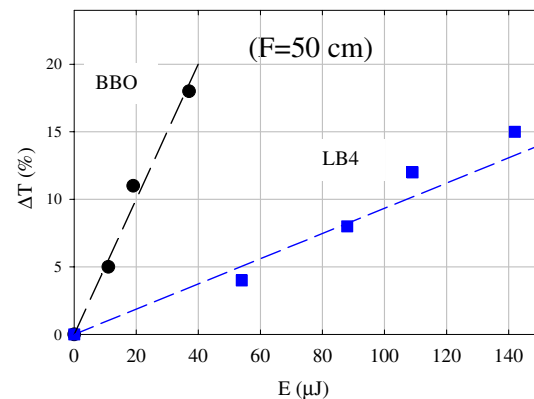


Fig. 3. (Color online) Comparison of NLA in BBO and LB4 crystals under UV irradiation ($E \parallel c$) based on z-scan measurements using the same experimental set-up. ΔT is defined as the difference between the maximum and the minimum transmission in z-scan curves measured at different levels of excitation pulse energy. The incident beam diameter used in the experiments is from 43 to 64 mm and is within Raleigh range.

of NLA coefficient at the fourth harmonic of the Nd:YAG laser operating at 10-Hz repetition rate. Since LB4 has negligible linear absorption at the fourth (266 nm) and second (532 nm) harmonic wavelengths (as can be seen in Fig. 1), initial creation of transient defects or color centers could occur due to TPA. These defects may induce single-photon absorption in the UV, green and IR spectral regions. If the pulse repetition rate increases (from 100 ms to 30 μs) so that the pulse period becomes comparable with the lifetime of these transient defects (previously reported to be in the μs scale) then the population of defects could accumulate and grow.^{16,17)} In fact, the absorption increases as the repetition rate increases (Fig. 4). Since true TPA is observed only at low repetition rates less than 100 Hz, the mechanism of absorption at higher repetition rates is more complex and could be attributed to NLA in general. Figures 5(a) and 5(b) show that at high repetition rates, absorption is greatly influenced by the crystal temperature. The increase of crystal temperature (see Fig. 5) causes a significant reduction of NLA coefficients (~ 3 times). Thermal dephasing has been known to limit the efficiency of laser frequency conversion in non-linear crystals and was clearly observed during high-power generation of UV light.¹⁸⁾ A non-uniform temperature profile is always generated inside these crystals, both along and traverse to the direction of the laser beam, because of the intrinsic linear absorption and non-linear multi-photon absorption of intensive laser pulses. These temperature profiles induce a non-uniform refractive index that modifies

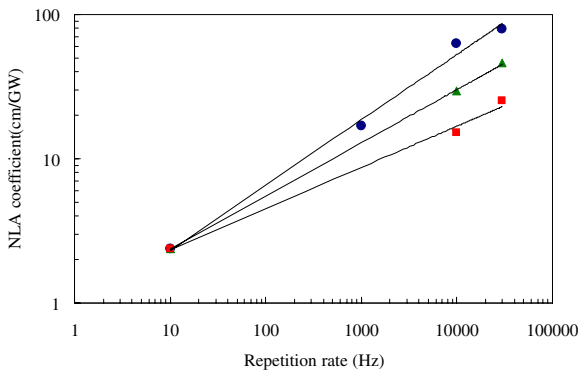
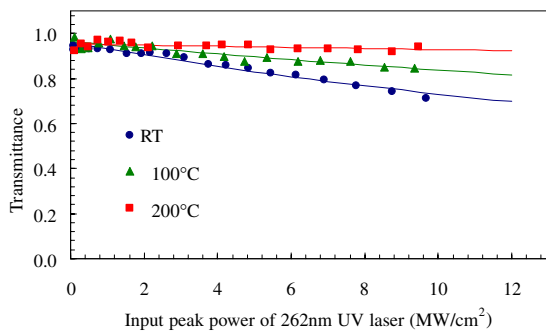
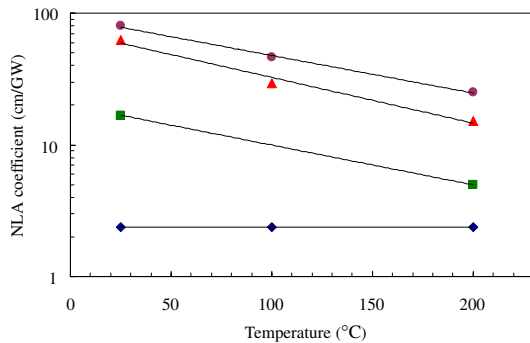


Fig. 4. (Color online) NLA coefficient in LB4 crystals vs the repetition rate at three different temperatures: rectangles: 200 °C, triangles: 100 °C, circles: RT).



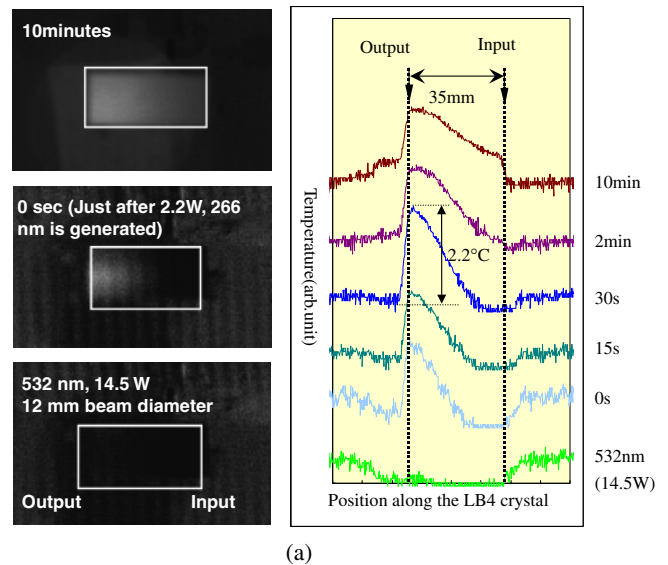
(a)



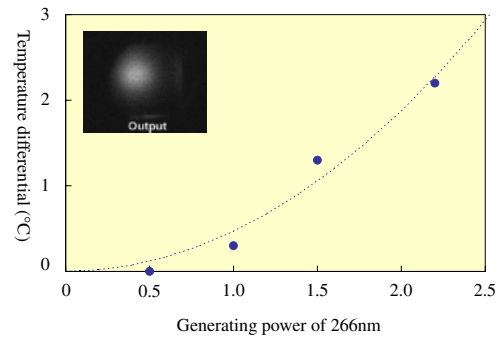
(b)

Fig. 5. (Color online) (a) Example of dependence of LB4 crystal transmission vs input power density at three different temperatures using UV laser excitation (262 nm, 10 kHz, 25 ns). Theoretical fit was used to determine the NLA coefficient at each temperature. (b) Temperature dependence of NLA coefficient in LB4 crystals at different repetition rates: rhombs: 10 Hz, rectangles: 1 kHz, triangles: 10 kHz, circles: 30 kHz.

the phase velocities of the laser beams; thereby resulting to a thermally induced phase mismatch. Beam scanning and *N*-plate harmonic generating are the methods that were proposed to alleviate this problem.^{19,20} The first method involved distribution of the thermal load to a large crystal area by either a moving laser beam or a mobile crystal holder while the second technique involved multiple thin plates of the crystals arranged in parallel with specified spacing between them. Both techniques are based on heat dissipation from the crystal by increasing the area exposed to air or a gas stream. A simpler approach would be to subject the heating profile generated from optical absorption to another profile that is reverse in temperature gradient; in effect compensat-



(a)



(b)

Fig. 6. (Color online) (a) Top view of the thermal image of LB4 crystal generating 2-W average power, 266-nm radiation at room temperature: The curves show the temperature gradient along the length of the crystal. Crystal heating, especially at the output end, occurs due to 532-nm conversion to UV. (b) The NLA-induced temperature differential at the output end of the crystal was measured to be $\sim 2.2^\circ$. Inset shows the thermal image at the output face.

ing the non-uniform temperature profile. By spatially overlapping these profiles that are opposite in temperature gradient, a uniform profile can always yield better phase matching. This can be achieved by heating up the crystal to induce a uniform temperature profile.

Moreover, a set of experiments where the LB4 crystals were used for the fourth harmonic generation of a high-repetition-rate (10 kHz) Nd:yttrium lithium fluoride (YLF) laser showed that at a higher temperature of 200 °C we were able to generate higher UV power as compared to operation at room temperature. This is a direct consequence of the reduction in NLA as well as the improvement of UV laser transmittance, as can be seen in Fig. 5.

The thermal image of the LB4 crystal producing UV output via frequency doubling of the 532 nm input was measured with a mid-infrared camera. Figure 6 shows the temperature gradient along the length of the crystal (the pump 532-nm beam is propagating from left to right). The temperature increase in the crystal is clearly observed towards the output end. This non-uniform temperature distribution indicates the absorption of mostly the fourth harmonic. The temperature differential induced by NLA was measured to be $\sim 2.2^\circ$. As mentioned above, non-uniform

heat generation during harmonic generation in LB4 is a critical issue that affects the phase matching conditions due to the change of the crystal refractive indicia with temperature. Obviously, improvement of the UV generation process requires the reduction of this absorption.

3. Conclusions

In conclusion, the relationship between the pulse repetition rate and crystal temperature with NLA, which is a limiting factor for frequency conversion in LB4, is investigated. Results show that NLA effects are reduced and crystal transparency is improved by using lower repetition rate lasers and by heating the harmonic generator crystal. At repetition rates above 1 kHz, the increase of NLA in LB4 crystals becomes a significant factor and should be taken into account in the design of UV generation stages with improved efficiency and long-term stability, particularly for fourth harmonic generation of Nd lasers.

- 1) Z. Liu, T. Kozeki, Y. Suzuki, N. Sarukura, K. Shimamura, T. Fukuda, M. Hirano, and H. Hosono: *Opt. Lett.* **26** (2001) 301.
- 2) C. T. Chen, B. C. Wu, A. D. Jiang, and G. M. You: *Sci. Sin. B* **28** (1985) 235.
- 3) C. T. Chen, Y. Wu, A. Jiang, G. You, R. Li, and S. Lin: *J. Opt. Soc. Am. B* **6** (1989) 616.
- 4) Y. Mori, I. Kuroda, S. Nakajima, T. Sasaki, and S. Nakai: *Appl. Phys. Lett.* **67** (1995) 1818.
- 5) R. Komatsu, T. Sugawara, K. Sassa, N. Sarukura, Z. Liu, S. Izumida, Y. Segawa, S. Uda, T. Fukuda, and K. Yamanouchi: *Appl. Phys. Lett.* **70** (1997) 3492.
- 6) Y. K. Yap, T. Inoue, H. Sakai, Y. Kagebayashi, Y. Mori, T. Sasaki, K. Deki, and M. Horiguchi: *Opt. Lett.* **23** (1998) 34.
- 7) P. Kumbhakar and T. Kobayashi: *Appl. Phys. B* **78** (2004) 165.
- 8) T. Sasaki, Y. Mori, M. Yoshimura, Y. K. Yap, and T. Kamimura: *Mater. Sci. Eng. R* **30** (2000) 1.
- 9) L. Isaenko, A. Dragomir, J. McInerney, and D. Nikogosyan: *Opt. Commun.* **198** (2001) 433.
- 10) R. W. Whatmore, N. M. Shorrocks, C. O'hara, F. W. Ainger, and I. M. Young: *Electron. Lett.* **17** (1981) 11.
- 11) Y. Suzuki, S. Ono, H. Murakami, T. Kozeki, H. Ohtake, N. Sarukura, G. Masada, H. Shiraishi, and I. Sekine: *Advanced Solid-State Laser Tech. Dig., WC4* 2002.
- 12) W. Zhou, H. Adachi, Y. Mori, T. Sasaki, and S. Nakai: *Tech. Rep. IEICE LQE95-24*, No. 113 (1995) 49.
- 13) M. Sheik-Bahae, A. A. Said, T. H. Wei, D. J. Hagan, and E. W. Van Stryland: *IEEE J. Quantum Electron.* **26** (1990) 760.
- 14) Li Heping, Zhou Feng, Zhang Xuejun, and Ji Wei: *Opt. Commun.* **144** (1997) 75.
- 15) R. DeSalvo, A. A. Said, D. J. Hagan, E. W. Van Stryland, and M. Sheik-Bahae: *IEEE J. Quantum Electron.* **32** (1996) 1324.
- 16) I. N. Ogorodnikov, V. Yu. Yakovlev, and L. I. Isaenko: *Radiat. Meas.* **38** (2004) 659.
- 17) I. N. Ogorodnikov and V. Yu. Yakovlev: *Phys. Status Solidi C* **2** (2005) 641.
- 18) Y. K. Yap, M. Inagaki, S. Nakajima, Y. Mori, and T. Sasaki: *Opt. Lett.* **21** (1996) 1348.
- 19) D. T. Hon and H. Bruesselbach: *IEEE J. Quantum Electron.* **16** (1980) 1356.
- 20) D. Eimerl: *IEEE J. Quantum Electron.* **23** (1987) 575.